A Novel Slicing Method for Thin Supercapacitors

*Hao Sun, Xuemei Fu, Songlin Xie, Yishu Jiang, Guozhen Guan, Bingjie Wang, Houpu Li, and Huisheng Peng**

Modern electronics has witnessed the rapid advancement of flexible and miniature devices in recent years, and meanwhile accelerated the development of the related energy storage systems.[1] To this end, thin energy storage devices have demonstrated promises in a variety of applications including miniature robotics, implanted microelectronics, and wearable electronics.[1–12] Several fabrication strategies including photolithography, sputtering, laser scribing, and chemical vapor deposition have been investigated.[13–26] For instance, Ajayan and co-workers fabricated micro-supercapacitors on hydrated graphite oxide films by the laser scribing method, i.e., laser-reduced graphite oxide was patterned with graphite oxide serving as a separator/electrolyte membrane, and a volumetric specific capacitance of ≈3.1 F cm^{-3} was achieved.[13] Müllen and co-workers developed all-solid-state graphene-based micro-supercapacitors via a micropatterning technique, and they showed a volumic specific capacitance of 17.9 F cm^{-3}.[18] Chen and co-workers produced all-solid-state ultrathin micro-supercapacitors based on graphene by combining photolithography with selective electrophoretic buildup.[21] The design for short diffusion pathways of the electrolyte promoted the realization of high weight specific capacitance of 285 F g^{-1}. In spite of these inspiring achievements, it remains challenging to realize neat and low-cost fabrication of thin energy storage devices and decrease their individual variations to the greatest extent.

A slicing technique using a sharp blade to cut bulk materials into thin slices represents a general and efficient method and has been adopted in various fields. In daily life, for instance, a variety of food materials can be cut into thin slices for cooking via a manual slicing process; in biological and medical sciences, ultrathin slices of tissues and organs can be obtained using a microtome for pathology detection.[27,28] Demonstrating several attractive advantages including low cost, controllable thickness, and small individual variation, the slicing method may well meet the requirements of next-generation thin energy storage devices. However, it is rare to use this method for developing microelectronic devices as there remain several challenges including the difficulty in selecting suitable materials, instability for the interface among different components, and complexity in the design of device structure.

Herein, a new slicing method is developed for fabricating thin supercapacitors with low cost and individual variation. The thin supercapacitors are tunable in thickness and demonstrate uniform surfaces and compact interfaces for excellent electrochemical properties; e.g., a high specific capacitance of 248.8 F g^{-1} (150.8 F cm^{-3}) has been achieved. They have been further demonstrated to effectively power commercial electronic devices. This slicing method can be generalized to fabricate the other thin energy and electronic devices with high performances.

The fabrication of the thin supercapacitor is illustrated in **Figure 1** and in the "Experimental Section." Briefly, patterned electrode and electrolyte are embedded into a supporting material, followed by cutting into the thin supercapacitor that is composed of a large number of supercapacitor units. The thickness of the thin supercapacitor can be accurately controlled from tens of nanometers to micrometers based on the well-developed slicing technology. For the study demonstration, aligned multiwalled carbon nanotube (MWCNT) arrays that are synthesized by chemical vapor deposition have been pressed down here along one direction to serve as the electrode; poly(vinyl alcohol) (PVA)/H_3PO_4 is incorporated as the gel electrolyte; and epoxy resin functions as the supporting material.

The dependence of the electrical property on the slicing angle in relative to the aligned MWCNT was first investigated for the MWCNT/epoxy resin composite (**Figure 2**a). For a composite with the length of 5 mm, width of 130 μm, and thickness of 40 μm, the electrical resistance was continuously increased from 1.2 to 4.4 kΩ with the increasing angle from 0° to 90° as more boundaries had been formed for the charge transport. In particular, when the MWCNTs were cut along their aligned directions with an angle of 0°, the electrons can rapidly and effectively transport along the length of MWCNTs; in contrast, when the slicing direction was perpendicular to the MWCNT length at 90°, the electrons have to transport among a large number of boundaries among MWCNTs with much higher resistances. Therefore, a cutting angle of 0° was studied unless specified otherwise. The resistance can also be tuned by varying the thickness of the sliced electrode, e.g., 5.4 and 0.9 kΩ at 10 and 60 μm with the same electrode length of 5 mm and width of 130 μm, respectively (Figure 2b).

The morphology and electronic properties of the electrodes were then investigated. The MWCNT electrode shared a width of ≈130 μm (Figure S1a, Supporting Information) with a compact contact with epoxy resin at the interface (Figure S1b, Supporting Information). The alignment of MWCNTs along the length direction of the electrode was well maintained to provide

H. Sun, X. Fu, S. Xie, Y. Jiang, Dr. G. Guan, Dr. B. Wang, H. Li, Prof. H. Peng
State Key Laboratory of Molecular Engineering of Polymers
Department of Macromolecular Science
Laboratory of Advanced Materials
Fudan University
Shanghai 200438, China
E-mail: penghs@fudan.edu.cn

DOI: 10.1002/adma.201600506

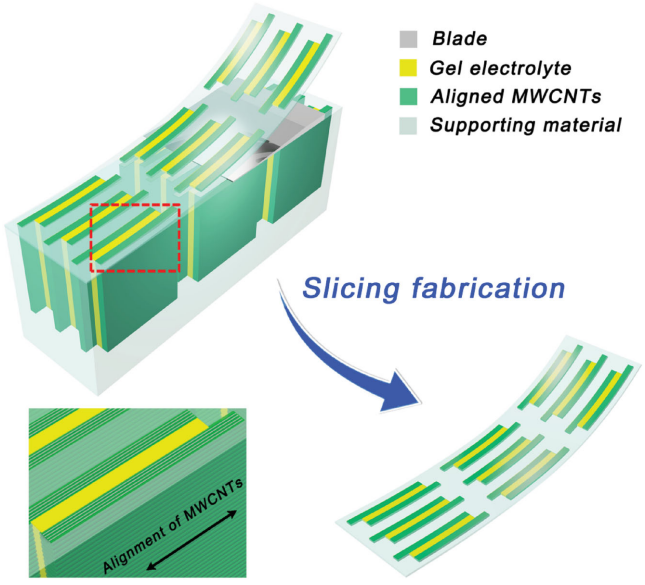

Figure 1. Schematic illustration to the fabrication of the thin supercapacitor through a slicing method. The left bottom image indicating the alignment of MWCNTs corresponds to the amplified area of the dashed rectangle.

high electrical conductivities ranged from 10^2 to 10^3 S cm^{-1}, which favor electron transports in electronic devices (Figure S1c, Supporting Information). The electrical conductivity can be further enhanced by depositing conducting polymers such as polyaniline (PANI). For the aligned MWCNT electrode, electrons hop from one MWCNT to the neighboring others based on a 3D hopping mechanism;[29,30] the electrical resistance of the MWCNT electrode mainly comes from the contact resistance among MWCNTs, and the conducting polymer chains serve as conducting pathways among neighboring MWCNTs.[5]

Both bare MWCNT and MWCNT/PANI composite electrodes are flexible. When a sliced MWCNT electrode was bent with increasing bending angles from 0° to 150°, the electrical resistance was varied within 3% (Figure 2c). After bending (at 90°) for 4000 cycles, no significant decreases on the resistance had been observed, which was beneficial for flexible electronic applications (Figure 2d). As a demonstration, a sliced MWCNT film served as a conductor to form a circuit which was composed of a commercial light-emitting diode (LED) (Figure 2e,f and Video S1, Supporting Information). The brightness of the LED remained almost unchanged when the MWCNT film was bent with various angles or deformed into different shapes.

This slicing method enabled a controllable fabrication in tuning the device thickness from nanometer to micrometer. At the present system, thin supercapacitors with thicknesses from several to tens of micrometers could be easily produced (Figure S2, Supporting Information), and the thickness ranged from 10 to 60 μm had been mainly studied in the following discussion. For the thin supercapacitor, the gel electrolyte was closely contacted with the aligned MWNCTs, which helped us to enhance the contact between the electrode and electrolyte (**Figure 3**a). A close contact between the electrode and epoxy resin was also verified (Figure 3b), which was important for a stable performance. Otherwise, the thin supercapacitor may easily break under bending with an interfacial stress force. Furthermore, a 3D surface topography of the thin supercapacitor was characterized by a laser scanning confocal microscopy, and it exhibited a uniform thickness without obvious defects at the interface (Figure 3c,d), which is important for high-performance electronic devices. The uniform surface and compact interface are attributed to the good compatibility of the building components.

The electrochemical properties of the supercapacitors based on the bare MWCNT were studied by galvanostatic charge–discharge measurements at increasing current densities. A symmetrical triangle shape was shared with high rate performance and a specific capacitance of 49.1 mF cm^{-2} at 1 mA cm^{-2} (Figure S3a, Supporting Information). The symmetrical rectangle shape in the cyclic voltammogram indicated reversible charge–discharge processes (Figure S3b, Supporting Information). As expected, the specific capacitances were varied in less than 1% after 2000 cycles (Figure S4, Supporting Information). The stable electrochemical performance at increasing current densities was important for a variety of applications.

The dependence of specific capacitances on slicing speed had been then investigated (**Figure 4**a). The specific capacitances of thin supercapacitors based on bare MWCNTs were first increased from 10.3 to 12.8 F g^{-1} with the increasing slicing speed from 2 to 20 mm s^{-1}, and remained almost unchanged with the further increase of the slicing speed to 75 mm s^{-1} (Figure 4b). It may be attributed to the relaxation of polymer chain in the gel electrolyte which affects the interface with MWCNTs at different slicing speeds. The relaxation of polymer chain is limited at higher slicing speeds, so the thin supercapacitor demonstrates a better interface between the MWCNT and gel electrolyte with lower internal resistance. This phenomenon was also verified by the decreasing internal resistance drop in the galvanostatic charge–discharge curves with increasing slicing speeds from 2 to 20 mm s^{-1} (Figure 4a). The improvement on the above interface reached a platform with the further increase in the slicing speed, so the specific capacitance was not obviously changed. Therefore, a slicing speed of 20 mm s^{-1} was mainly studied and discussed below.

Besides the improvement in the electrical conductivity, the introduction of PANI also largely increases the specific capacitance of the supercapacitor. For the MWCNT/PANI composite electrode, reversible charge–discharge performances at a variety of scan rates and current densities were achieved (Figure 4c and Figure S5, Supporting Information), and a higher specific capacitance of ≈240 F g^{-1} (145.5 F cm^{-3}) was obtained, which was ≈20 times higher than the bare MWCNT. The performance enhancements can be ascribed to the following reasons. First, the highly aligned MWCNTs provide both conductive pathways for rapid electron transport and ideal porous networks for the incorporation of PANI. Second, the uniformly coated PANI on the surfaces of MWCNTs provides high pseudocapacitance that largely enhances the energy storage (Figure S6, Supporting Information). Third, the stable interface among different components contributes to maintaining the integrity of the morphology and structure, thus well retaining the high specific

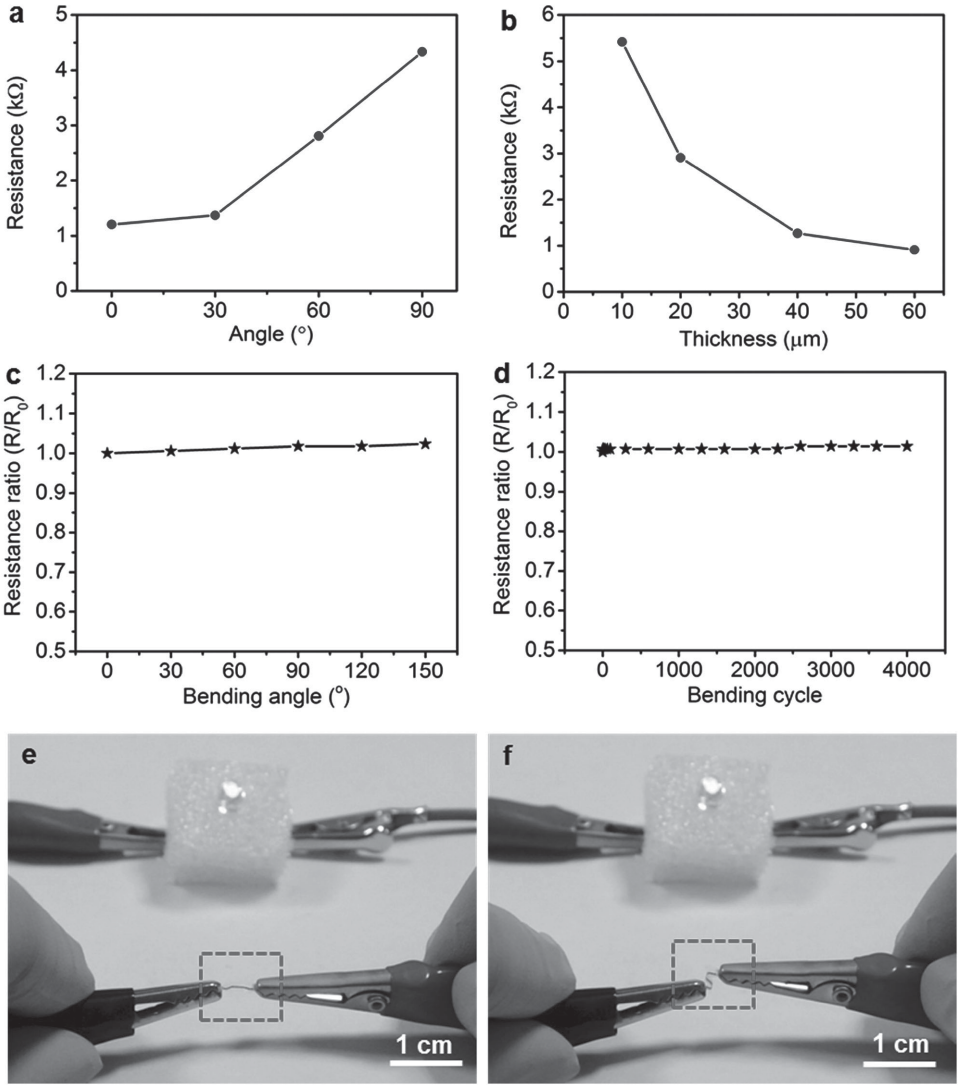

Figure 2. a,b) Dependence of electrical resistance on the slicing angle (a) and the thickness (b) of the aligned MWCNT/epoxy resin composite. The composite showed a length of 5 mm, width of 130 μm, and thickness of 40 μm in panel (a). The length and width were the same of 5 mm and 130 μm in panel (b), respectively. c,d) Dependence of electrical resistance on bending angle and cycle, respectively. R_0 and R correspond to the resistances before and after bending, respectively. The composite showed a length of 5 mm, width of 130 μm, and thickness of 40 μm. The bending angle in panel (d) was 90°. e,f) Photographs of a sliced MWCNT/epoxy resin (with a length of 5 mm, a width of 130 μm, and a thickness of 20 μm) being connected to a circuit containing an LED and power source (e) and under deformation (f).

capacitance of 252.5 F g^{-1} before slicing. For the MWCNT/PANI composites with the increasing thickness from 10 to 60 μm, the galvanostatic charge–discharge characterization was compared at the same current density of 0.50 A g^{-1} (Figure 4d), and it was found that the specific capacitances remained almost unchanged with a maximal value of 248.8 F g^{-1} (150.8 F cm^{-3}) at 40 μm (Figure 4e). The cyclic stability of the thin supercapacitor had been further verified by a cyclic charge–discharge characterization, and the specific capacitance can be maintained by 96.0% after 2000 cycles (Figure S7, Supporting Information). The energy and power densities reached 3.10 mW h cm^{-3} and 0.99 W cm^{-3}, respectively, which were comparable to the previous reports on miniature energy storage devices and commercial counterparts (Figure 4f).[4,5,15,22]

The slicing method shows several unique advantages that are favored in practical applications. First, the individual variation of the obtained thin supercapacitors can be reduced to the greatest extent. For 22 thin supercapacitors produced under the same condition, the specific capacitance and internal resistance were varied within 8.8% and 11.6%, respectively (**Figure 5**a–c). Second, the thin supercapacitors exhibit a low areal density of ≈0.26 mg cm^{-2}, which is comparable to the state-of-the-art thin energy storage devices that are promising for lightweight and thin electronic devices.[24] Third, the high flexibility of the thin supercapacitor is favorable for flexible electronics. The specific capacitance can be maintained by 91% with increasing bending angles from 0° to 180° (Figure S8, Supporting Information); it was retained by 96% after bending

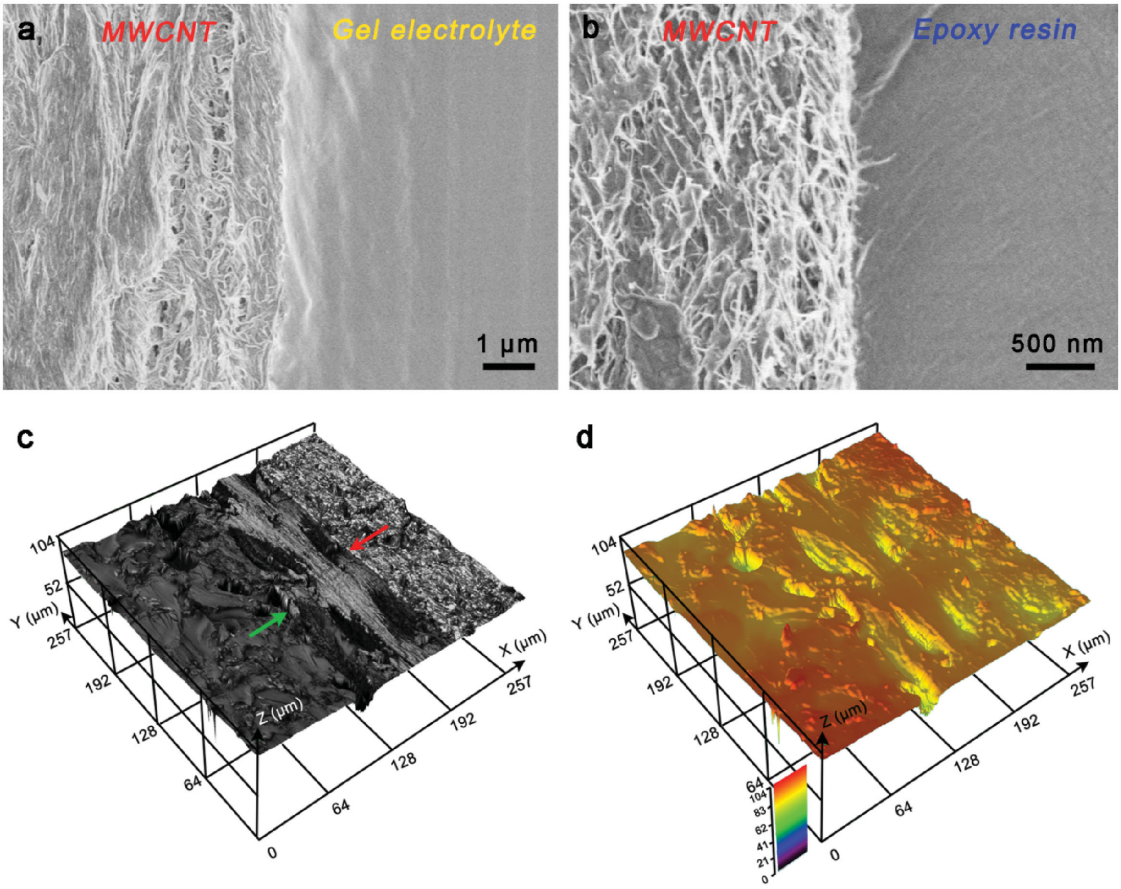

Figure 3. Morphology characterization of the thin supercapacitor. a) The interface composed of MWCNT and gel electrolyte. b) The interface composed of MWCNT and epoxy resin. c,d) Confocal 3D laser image and height map of the interface of the thin supercapacitor. The top right and bottom left arrows in panel (c) indicate the interfaces of panels (a) and (b), respectively.

(at 90°) for 300 cycles (Figure S9, Supporting Information). Last but not the least, the slicing method enables tunable connection that can be designed to tune the output voltage and energy. For instance, a thin supercapacitor with three units can be connected in series or parallel (Figure 5d), and the output voltage and discharge time were accordingly increased by three times (Figure 5e). As an application demonstration to reveal the mentioned advantages, a thin supercapacitor with three in-series units was fixed on a fingernail (Figure 5f) to light up a commercial LED (Figure 5g and Video S2, Supporting Information), suggesting the high potential of the thin supercapacitors as lightweight, thin, and flexible power sources.

In conclusion, a general and effective slicing method is developed for fabricating thin supercapacitors with low cost and individual variation. The thin supercapacitors exhibit uniform surfaces and compact interfaces with well controlled thicknesses. A high specific capacitance of 248.8 F g^{-1} (150.8 F cm^{-3}) has been achieved with tunable output voltage and energy. They are demonstrated as lightweight, thin, and flexible power sources to drive commercial electronics. This slicing method is also compatible for fabricating a variety of other devices including sensors, transistors, solar cells, and batteries aiming at large-scale production and high performances.

Experimental Section

Preparation of Aligned Bare MWCNT and MWCNT/PANI Composite Films: Aligned MWCNT arrays with an average height of 1 mm were vertically grown on silicon wafer via a chemical vapor deposition. These arrays were pressed down toward one direction by a precleaned glass slide and then peeled off from the substrate by a sharp blade.[31,32] To prepare an aligned MWCNT/PANI composite, the above bare MWCNT film was immersed in an aqueous electrolyte containing 0.1 M aniline and 1 M sulfuric acid, followed by electrochemical deposition at a potential of 0.75 V using platinum wire (CHI115, a diameter of ≈0.5 mm) and Ag/AgCl electrode (CHI111, a diameter of 4 mm) as counter and reference electrodes, respectively.[33] The weight percentage of PANI was 70% which was controlled by assuming an average 2.5 electrons per aniline monomer. The resulting composite film was further washed with deionized water for two times and dried in air prior to the use.

Fabrication of Sliced Thin Supercapacitors: Aligned MWCNT or MWCNT/PANI composite films were coated with PVA/H_3PO_4 gel electrolyte and vacuumized for 10 min to enhance the electrolyte infiltration into the electrodes. The above process was repeated for at least two times. The same two film electrodes were stacked together along the MWCNT-aligned direction to form a thin film supercapacitor. Each electrode shared a width of ≈110 μm and the distances between two electrodes were ranged from 400 to 600 μm. The weight of active materials (MWCNT and PANI) was ≈3.3 mg for a 0.25 cm^2 device. The stacked two films were successively immersed in mixtures with different volume ratios of acetone and embedding solution (2/1 for 3 h, 1/1 for 12 h, 1/2 for 3 h, and pure embedding solution for 24 h). The embedding

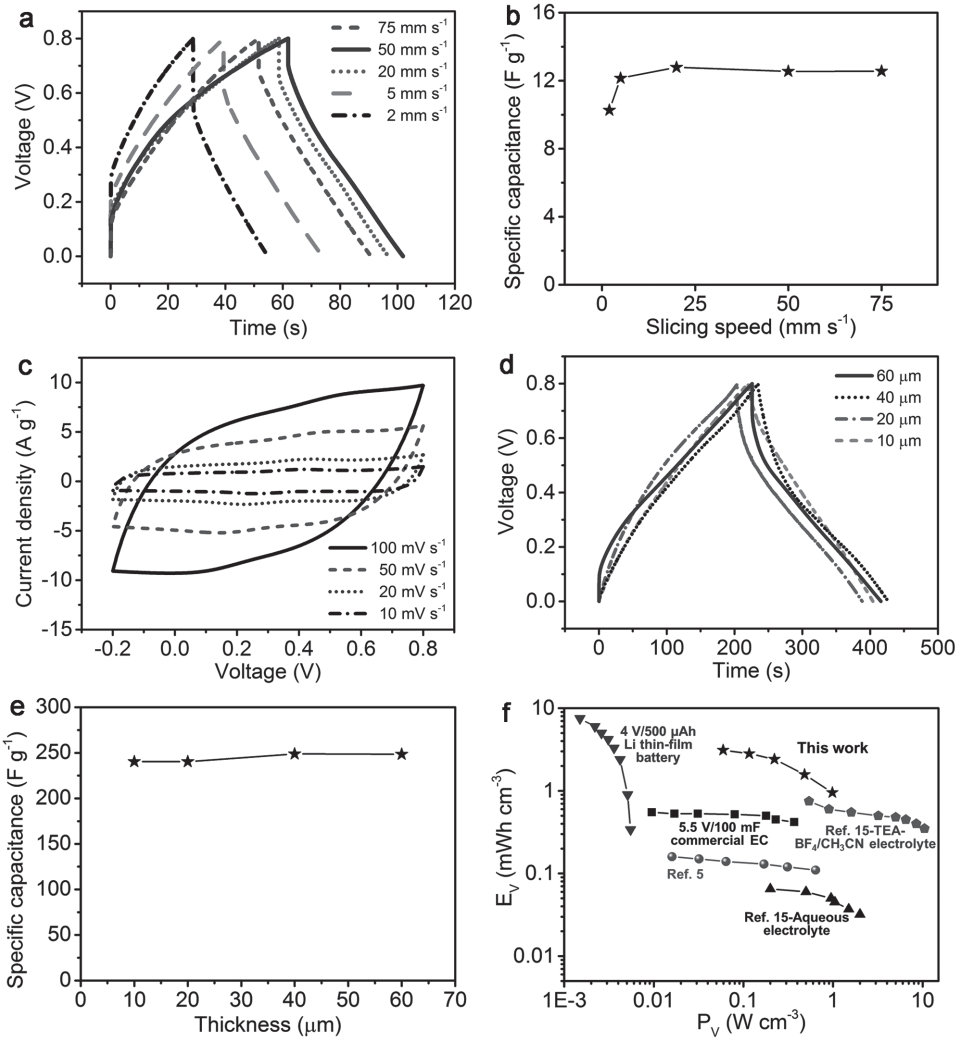

Figure 4. Electrochemical properties of the thin supercapacitor. a) Galvanostatic charge–discharge curves for bare MWCNT electrodes with increasing slicing speeds from 2 to 75 mm s^{-1} at a current density of 0.15 A g^{-1}. b) Dependence of specific capacitance on slicing speed. c) Cyclic voltammograms for MWCNT/PANI electrodes at different scan rates. d) Galvanostatic charge–discharge curves for thin supercapacitor derived from aligned MWCNT/PANI composite electrodes with increasing thicknesses from 10 to 60 μm at a current density of 0.50 A g^{-1}. e) Dependence of specific capacitance on the thickness of the thin supercapacitor. f) Comparison of energy and power densities with the other energy-storage devices.

solution was prepared by mixing epoxy resin (SPI-PON 812) with additives including T-168 (Shenyang Southeast Chemical Institute) as a flexibilizer, dodecenyl succinic anhydride and methyl-5-norbornene-2,3-dicarboxylic anhydride (SPI Supplies Division of Structure Probe, Inc.) as curing agents, and 2,4,6-tris (dimethylaminomethyl phenol) (SPI Supplies Division of Structure Probe, Inc.) as a curing catalyst, followed by a vacuum treatment to exclude air bubbles.[34] It was then placed in a ribbon-shaped mold containing an embedding solution, followed by curing at 60 °C for 24 h. The resulting sample was removed from the mold and fixed on the sample stage of a microtome. A tungsten carbide disposable blade (Leica TC65, a length of 65 mm) was used to cut it along the MWCNT-aligned direction.

The stiffness of the MWCNT/epoxy block was characterized by compression strength, which can be tuned by varying the weight percentage of the flexibilizer. Weight percentages of 0%, 10%, 15%, and 30% corresponded to compressive strengths of 810, 1022, 1174, and 785 MPa, respectively. Low flexibilizer contents led to low compressive strengths and reduced the maximal thickness of the slices. For instance, an MWCNT/epoxy resin block with 5% flexibilizer produced thin supercapacitors with a maximal thickness of 60 μm, and larger thicknesses may cause the cracking of the block due to its high brittleness. A higher content such as 30% resulted in the extraction of some epoxy resin out of the block during the slicing process due to the enhanced toughness. As a result, weight percentages between 10% and 20% were suitable for slicing, and a weight percentage of 15 % was mainly used in this work.

Calculation of Specific Capacitance and Energy and Power Densities: The capacitance (C) was calculated from the equation of $C = 2 \times (I \times \Delta t)/\Delta V$, where I, Δt, and ΔV correspond to the discharge current, discharge time, and operating voltage window, respectively. The mass (C_M) and volumetric (C_V) specific capacitances were calculated by dividing the capacitance by the mass and volume of one electrode, respectively. The volumetric (E_V) energy densities were calculated from the equation of $E_V = C_V \times \Delta V^2/(8 \times 3600)$. The volumetric ($P_V$) power density was calculated from the equation of $P_V = E_V \times 3600/\Delta t$.

Characterization: The structures were characterized by the laser scanning confocal microscope (Olympus LEXT OLS4100) and scanning electron microscopy (Hitachi FE-SEM S-4800 operated at 1 kV).

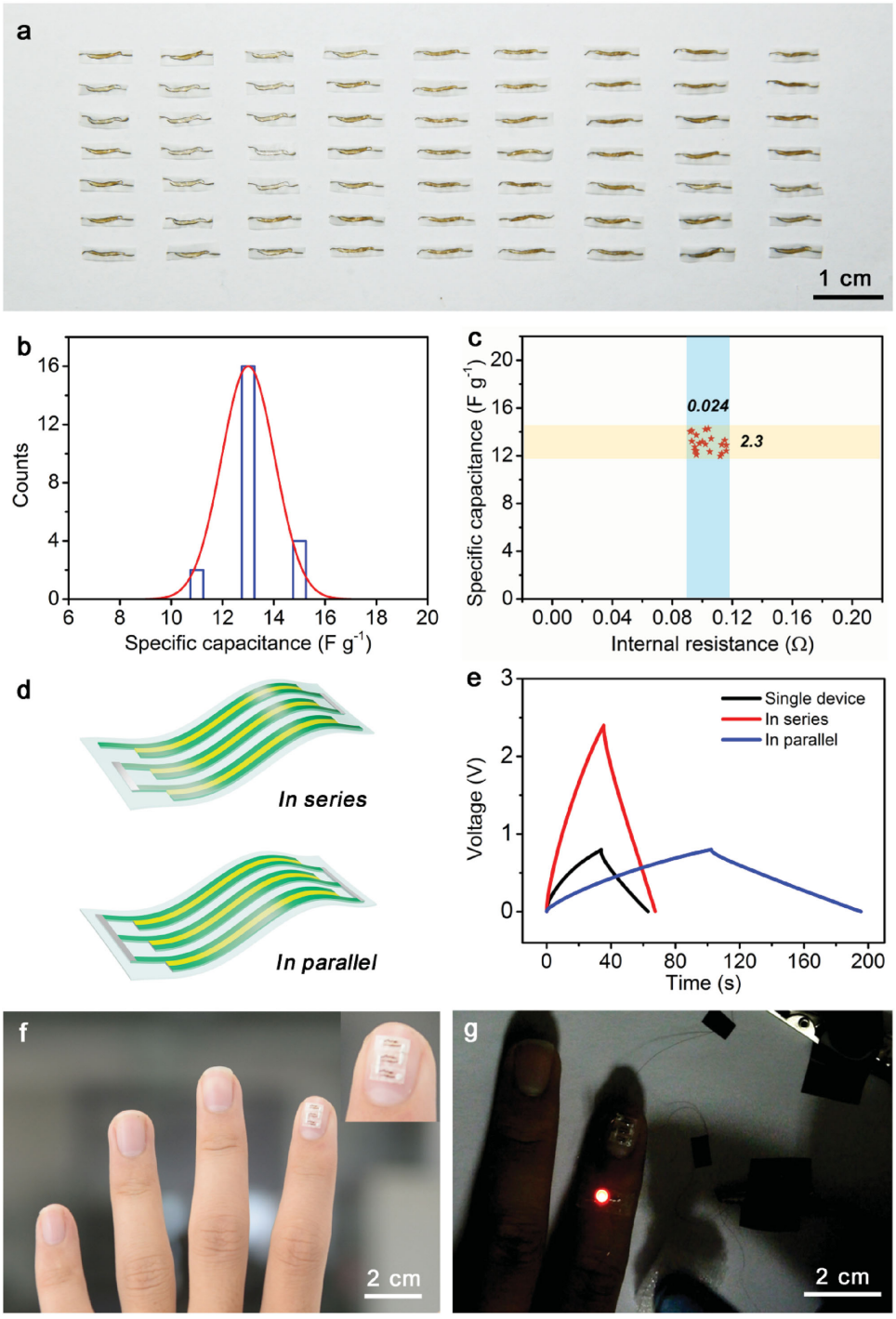

Figure 5. a) Photograph of the thin supercapacitor (a thickness of 20 μm and a length of 5 mm for each unit). b) Histogram of the specific capacitance of 22 thin supercapacitors under the same fabrication condition. c) Comparison of the specific capacitance and internal resistance of 22 thin supercapacitors in panel (b). d) Schematic illustration to two connections in series and parallel. e) Galvanostatic charge–discharge curves of one unit and three units connected in series and parallel. f) Photograph of three units connected in series and placed on a fingernail. g) The thin supercapacitors in panel (f) powering a red-light-emitting diode in the dark.

The electrode widths were measured using an optical microscope (Olympus BX51). The thin supercapacitor was made using a microtome (Leica RM2265). The thicknesses were measured using a stylus profilometer (Veeco Dektak 150). The compression strengths were measured using an electronic universal testing machine (CMT4104) with a compressing speed of 20 mm min^{-1}. Electrical resistances were calculated using a Keithley 2400 Source Meter. Electrochemical measurements and depositions were performed on an electrochemical workstation (CHI 660E). The cyclic stability was characterized by Arbin electrochemical testing system (MSTAT-5 V/10 mA/16Ch).

Supporting Information

Supporting Information is available from the Wiley Online Library or from the author.

Acknowledgements

H.S. and X.F. contributed equally to this work. This work was supported by NSFC (Grant Nos. 21225417, 51573027, and 51403038), STCSM (Grant Nos. 15XD1500400, 12nm0503200, and 15JC1490200), and the Program for Outstanding Young Scholars from Organization Department of the CPC Central Committee.

Received: January 27, 2016
Revised: March 1, 2016
Published online: May 17, 2016

[1] M. Beidaghi, Y. Gogotsi, *Energy Environ Sci.* **2014**, *7*, 867.
[2] J. Chmiola, C. Largeot, P. Taberna, P. Simon, Y. Gogotsi, *Science* **2010**, *328*, 480.
[3] D. Yu, K. Goh, Q. Zhang, L. Wei, H. Wang, W. Jiang, Y. Chen, *Adv. Mater.* **2014**, *26*, 6790.
[4] J. Ren, L. Li, C. Chen, X. Chen, Z. Cai, L. Qiu, Y. Wang, X. Zhu, H. Peng, *Adv. Mater.* **2013**, *25*, 1155.
[5] H. Sun, X. You, J. Deng, X. Chen, Z. Yang, J. Ren, H. Peng, *Adv. Mater.* **2014**, *26*, 2868.
[6] X. Dong, Z. Guo, Y. Song, M. Hou, J. Wang, Y. Wang, Y. Xia, *Adv. Funct. Mater.* **2014**, *24*, 3405.
[7] D. Yu, K. Goh, H. Wang, L. Wei, W. Jiang, Q. Zhang, L. Dai, Y. Chen, *Nat. Nanotechnol.* **2014**, *9*, 555.
[8] D. Yu, S. Zhai, W. Jiang, K. Goh, L. Wei, X. Chen, R. Jiang, Y. Chen, *Adv. Mater.* **2015**, *27*, 4895.
[9] W. Jiang, S. Zhai, Q. Qian, Y. Yuan, H. E. Karahan, L. Wei, K. Goh, A. K. Ng, J. Wei, Y. Chen, *Energy Environ. Sci.* **2016**. *9*, 611.
[10] D. Yu, Q. Qian, L. Wei, W. Jiang, K. Goh, J. Wei, J. Zhang, Y. Chen, *Chem. Soc. Rev.* **2015**, *44*, 647.
[11] M. Yu, Y. Han, X. Cheng, L. Hu, Y. Zeng, M. Chen, F. Cheng, X. Lu, Y. Tong, *Adv. Mater.* **2015**, *27*, 3085.
[12] M. Yu, Y. Zhang, Y. Zeng, M. S. Balogun, K. Mai, Z. Zhang, X. Lu, Y. Tong, *Adv. Mater.* **2014**, *26*, 4724.
[13] W. Gao, N. Singh, L. Song, Z. Liu, A. L. M. Reddy, L. Ci, R. Vajtai, Q. Zhang, B. Wei, P. Ajayan, *Nat. Nanotechnol.* **2011**, *6*, 496.
[14] L. Cao, S. Yang, W. Gao, Z. Liu, Y. Gong, L. Ma, G. Shi, S. Lei, Y. Zhang, S. Zhang, R. Vajtai, P. Ajayan, *Small* **2013**, *9*, 2905.
[15] M. Kady, S. Veronica, D. Sergey, R. B. Kaner, *Science* **2012**, *335*, 1326.
[16] Q. Meng, H. Wu, Y. Meng, K. Xie, Z. Wei, Z. Guo, *Adv. Mater.* **2014**, *26*, 4100.
[17] K. Wang, W. Zou, B. Quan, A. Yu, H. Wu, P. Jiang, Z. Wei, *Adv. Energy Mater.* **2011**, *1*, 1068.
[18] Z. Wu, K. Parvez, X. Feng, K. Müllen, *Nat. Commun.* **2013**, *4*, 2487.
[19] Z. Wu, K. Parvez, A. Winter, V. H. Vieker, X. Liu, S. Han, A. Turchanin, X. Feng, K. Müllen, *Adv. Mater.* **2014**, *26*, 4552.
[20] D. Qi, Z. Liu, Y. Liu, W. Leow, B. Zhu, H. Yang, J. Yu, W. Wang, H. Wang, S. Yin, X. Chen, *Adv. Mater.* **2015**, *27*, 5559.
[21] Z. Niu, L. Zhang, L. Liu, B. Zhu, H. Dong, X. Chen, *Adv. Mater.* **2013**, *25*, 4035.
[22] S. Kim, H. Koo, A. Lee, P. Braun, *Adv. Mater.* **2014**, *26*, 5108.
[23] C. Meng, J. Maeng, S. John, P. Irazoqui, *Adv. Energy Mater.* **2014**, *4*, 1301269.
[24] Z. Su, C. Yang, B. Xie, Z. Lin, Z. Zhang, J. Liu, B. Li, F. Kang, C. P. Wong, *Energy Environ. Sci.* **2014**, *7*, 2652.
[25] M. Beidaghi, C. Wang, *Adv. Funct. Mater.* **2012**, *22*, 4501.
[26] M. Beidaghi, C. Wang, *Electrochim. Acta* **2011**, *56*, 9508.
[27] A. Igersheim, O. Cichocki, *Rev. Palaeobot. Palynol.* **1996**, *92*, 389.
[28] W. Han, S. Heo, T. Driscoll, J. Delucca, C. McLeod, L. Smith, R. Duncan, R. Mauck, D. M. Elliott, *Nat. Mater.* **2016**, *15*, 477; DOI:10.1038/nmat4520.
[29] T. Chen, S. Wang, Z. Yang, Q. Feng, X. Sun, L. Li, Z. S. Wang, H. Peng, *Angew. Chem. Int. Ed.* **2011**, *50*, 1815.
[30] H. Peng, M. Jain, D. E. Peterson, Y. Zhu, Q. Jia, *Small* **2008**, *4*, 1964.
[31] Z. Yang, L. Li, H. Lin, Y. Luo, R. He, L. Qiu, J. Ren, H. Peng, *Chem. Phys. Lett.* **2012**, *549*, 82.
[32] H. Sun, R. Che, X. You, Y. Jiang, Z. Yang, J. Deng, L. Qiu, H. Peng, *Adv. Mater.* **2014**, *26*, 8120.
[33] A. Yu, I. Roes, A. Davies, Z. Chen, *Appl. Phys. Lett.* **2010**, *96*, 253105.
[34] a) L. Li, Z. Yang, H. Gao, H. Zhang, J. Ren, X. Sun, T. Chen, H. G. Kia, H. Peng, *Adv. Mater.* **2011**, *23*, 3730; b) S. Huang, L. Li, Z. Yang, L. Zhang, H. Saiyin, T. Chen, H. Peng, *Adv. Mater.* **2011**, *23*, 4707.